Scheme I. Schematic Reaction Curves Showing the Redox Isomers of the RH + $M^{\bullet+}$ System

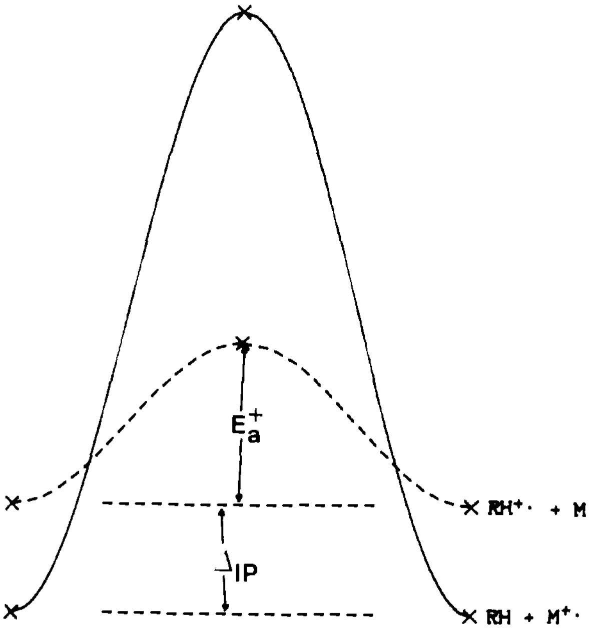

4 have a plane of symmetry through the C_3H_6 unit and that, therefore, the stereochemistry of the 1,3-shift is no longer defined. Figure 1 shows schematic reaction profiles illustrating the course of the 1,3-hydrogen shift reaction for the different metals.

The propene $Be^{\bullet+}$ complex $\mathbf{1}_{Be}$ is surprisingly stable. Symmetrical first row–first row odd-electron bonds typically have dissociation energies between 40 and 50 kcal mol^{-1},[7] and the ethylene Li^+ complex investigated previously[8] is bound by about 23 kcal mol^{-1}. The stability of the complexes **1** decreases in the order Be > Mg $\simeq$ Zn > Ca, as would be expected from the ionization potentials of the metals and the fact that odd-electron bond energies decrease on descending the periodic table.[7] The 1,2-shift transition states **2** lie 45 (Be) to 85 (Ca) kcal mol^{-1} higher in energy than the complexes **1**. The net activation energy (propene + $M^{\bullet+}$ → **2**) is negative for Be, 40–50 kcal mol^{-1} for Zn and Mg, and close to 80 kcal mol^{-1} for Ca. The 1,2-shift transition states **2** are the highest points on the reaction profile as the 1,3-beryllium shift in $\mathbf{3}_{Be}$ has an activation energy of only 6.5 kcal mol^{-1}. Although the activation energies (**1** → **2**) are substantial, there is nevertheless a significant catalysis of the overall 1,3-hydrogen shift by Be, Zn, and Mg.

The general principles of this type of catalysis are shown in Scheme I below. The two curves represent schematic reaction profiles for the total energies of the two redox isomers of the reacting system, RH + $M^{\bullet+}$ and $RH^{\bullet+}$ + M (for simplicity, it is assumed that there is little or no interaction between the organic moiety, RH, and the metal, M, although this will normally not be the case). The high activation energy for the reaction of neutral RH (solid line) compared to that of the radical cation reaction (dashed line) leads to a crossing of the two reaction profiles on approaching the transition state. This results in an internal electron transfer from RH to M as the system approaches the transition state and a net activation energy of $\Delta_{IP} + E_a^+$, where Δ_{IP} is the difference in activation energy between RH and the metal, and E_a^+ is the activation energy of the radical cation reaction. Table I shows that the calculated activation energies are, in fact, close to $\Delta_{IP} + E_a^+$ for Be and Zn. The complexation energy differences between the reactant and the transition state with the metal are ignored in this simplified treatment. Magnesium whose ionization potential is close to that of the transition state, to which it should thus complex strongly,[7] therefore gives a significantly lower activation energy than $\Delta_{IP} + E_a^+$. Note that for calcium Δ_{IP} is larger than the activation energy of the neutral reaction, so that the two curves never cross. The small degree of catalysis observed in this case is due to differences in complexation energy along the reaction path. The type of catalysis observed for Be, Mg, and Zn should be general and independent of the orbital characteristics of the metal and the organic substrate for all "hole-catalyzed" reactions. Interestingly, Ghosh and Kevan[15] have recently identified a $Pd^{\bullet+}$ ethylene complex as the immediate precursor for ethylene dimerization on NaPd–X zeolites. Ethylene dimerization, similar to the 1,3-hydrogen shift in propene, is a reaction that proceeds in the radical cation case but not for the neutral system.[1]

Acknowledgment. This work was supported by the Fonds der Chemischen Industrie and the Stiftung Volkswagenwerk and was facilitated by the generous support of the Convex Computer GmbH.

---

(15) Ghosh, A. K.; Kevan, L. *J. Phys. Chem.* **1988**, *92*, 4439.

Dehydrohalogenation of *vic*-Dibromoethanes Catalyzed by Iron

Angela R. Suárez,* María R. Mazzieri, and
Alejandra G. Suárez[1]

Departamento de Química Orgánica
Facultad de Ciencias Químicas
Universidad Nacional de Córdoba
Suc. 16 CC. 61-(5016)-Córdoba, Argentina

Received May 6, 1988

We describe here the dehydrobromination of 1,2-dibromo-1,1-diphenylethane in CCl_4 solution with freshly reduced powdered iron with a 2–7μ particle diameter as catalyst (eq 1).

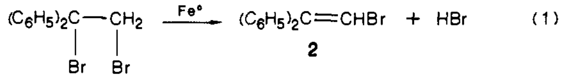

$$\underset{\text{Br}}{(C_6H_5)_2\overset{|}{C}}-\underset{\text{Br}}{\overset{|}{C}H_2} \xrightarrow{Fe^\circ} (C_6H_5)_2C{=}CHBr + HBr \qquad (1)$$

1 2

Reactions were carried out at several temperatures and monitored by ^1H NMR and UV–Vis spectroscopy. Blanck reactions yielded unchanged **1**. The ^1H NMR spectra revealed no changes in intensity of aromatic protons, but the sum of methylenic protons (M) from **1** and vinylic proton (V) from **2** decreased until a minimum, and then it increased again when more than 95% of **1** reacted. Correlations of a simple ratio of relative intensities of proton signals **1** – M/V + M as a function of **1** conversion (**1** – M) is expected to give a linear relationship. Figure 1 collects the results at different temperatures showing an important deviation zone that increased as the reaction temperatures diminished.

Figure 2 shows typical visible spectra of the reaction mixture, and Table I presents the relative absorbance intensities of the bands. The maximum occurred at the same values of **1** conversion as the deviation zone by ^1H NMR, suggesting a common mechanism for both results. The wavelengths observed are close to those of Fe^{III}-Br compounds[2] and those attributed to halogen → metal charge transfer.[3]

These observations could not be explained merely on the basis of the proposed dehydrohalogenation mechanisms: (i) homolysis of a carbon–halogen bond, followed by a β-hydrogen elimination and (ii) a β-hydrogen elimination from an initial carbenium ion.[4] Other β-elimination reactions are the known decomposition of metal–alkyl complexes leading to olefin formation.[5] Our results can be best understood if similar complexes were formed on the

---

(1) Grateful recipient of a fellowship from the Consejo Nacional de Investigaciones Científicas y Técnicas (CONICET), Argentina.

(2) Gregory, N. W. *J. Phys. Chem.* **1977**, *81* 1857.

(3) Hendrickson, D. N.; Kinnaird, M. G.; Suslick, K. S. *J. Am. Chem. Soc.* **1987**, *109*; 1243.

(4) Noller, H.; Kladnig, W. *Catal. Rev. Sci. Eng.* **1976**, *13*, 149.

(5) (a) Schrock, R. R.; Parshall, G. W. *Chem. Rev.* **1976**, *76*, 243. (b) Brookhart, M.; Green, M. L. H. *J. Organomet. Chem.* **1983**, *250*, 395. (c) Eisenstein, O.; Jean, J. *J. Am. Chem. Soc.* **1985**, *107*, 1186.

0002-7863/89/1511-0763$01.50/0

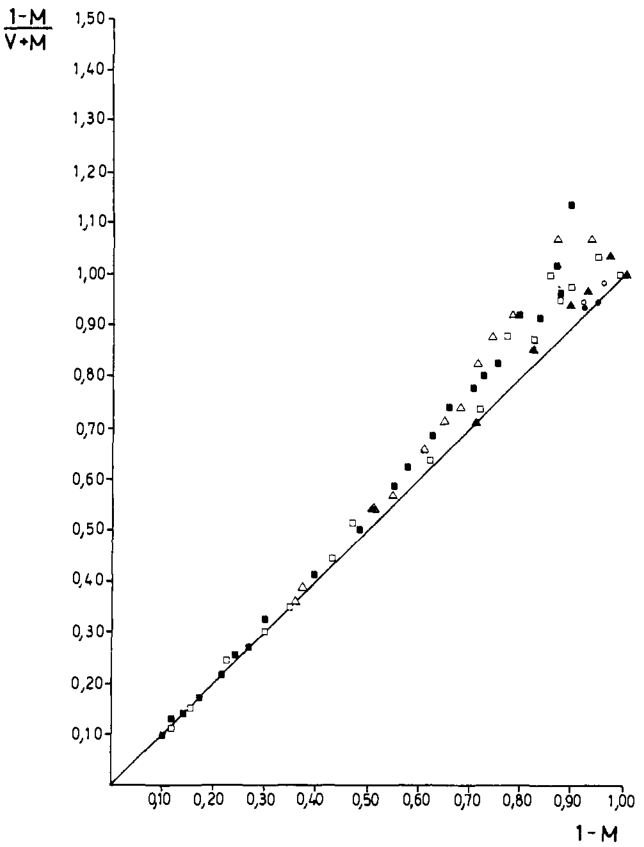

Figure 1. Correlation of relative intensities of proton signals and **1** conversion by ^{1}H NMR: M = methylenic signal, V = vinylic signal; temperatures (■) 30 °C, (△) 37 °C, (□) 50 °C, (▲) 76 °C, (●) performed at 30 °C and completed at 76 °C, (○) carried out at 37 °C and completed at 76 °C. Each point in the curve is the average from five to eleven reactions.

Table I. Relative Absorbances of the Visible Spectra Bands

1 conversion	relative intensities		
	I/II	III/II	II
0.06–0.12	0.97	0.30	1.00
0.13–0.40	0.94	0.31	1.81
0.55–0.74	0.93	0.35	7.45
0.75–0.94	0.86	0.59	18.49
0.95–1.00	0.92	0.51	9.63

active sites at the catalyst surface.

Steps (a) and (b) are the well-known reactions of HBr elimination and its further decomposition at the iron surface. In step (c), metal insertion intermediates are proposed. Similar structures have been postulated for positive[6] and negative iron insertion[7] to carbon–halogen bonds and for the decomposition of Grignard reagents catalyzed by $FeCl_3$.[8] Elimination of a β-hydrogen led to vinyl derivative **2** in step (e).

The difference in proton integration can be caused by "agostic" hydrogen atoms whose resonance may appear at high fields. Failure to detect them is attributable to several facts. First, the spectral data in Table I show that the absorbance intensity changes of bands I and III relative to band II demonstrate the existence of more than one species in solution. Second, the maximum difference in proton integration was about 0.2 mmol. Therefore, concentration of "agostic" hydrogens is too low to be detected by a CW NMR spectrometer.

The presence of organoiron compounds was demonstrated by column chromatography of reaction mixtures on silica gel with *n*-hexane–benzene as eluents. The mass spectra of fractions 4–6

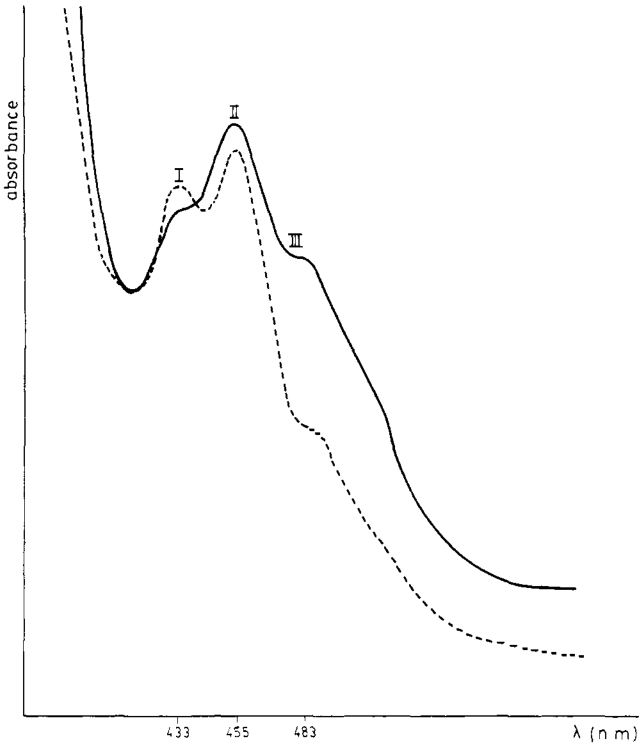

Figure 2. Typical visible absorption spectra of two different mixtures: (—) deviation zone, (---) completed reactions. Ratio of sample concentracions was 1:2.

Scheme I

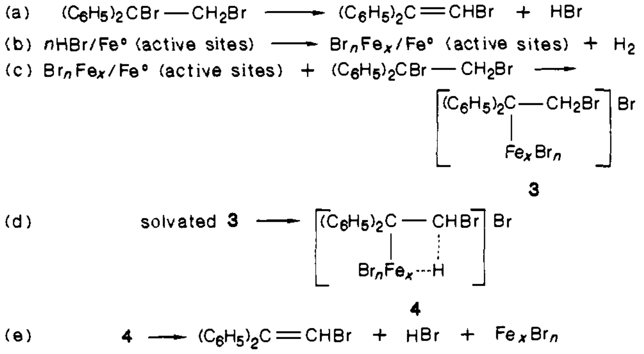

$$\text{(a)}\quad (C_6H_5)_2CBr{-}CH_2Br \longrightarrow (C_6H_5)_2C{=}CHBr + HBr$$

$$\text{(b)}\quad n\,HBr/Fe^\circ\ \text{(active sites)} \longrightarrow Br_nFe_x/Fe^\circ\ \text{(active sites)} + H_2$$

$$\text{(c)}\quad Br_nFe_x/Fe^\circ\ \text{(active sites)} + (C_6H_5)_2CBr{-}CH_2Br \longrightarrow \left[\begin{array}{c}(C_6H_5)_2C{-}CH_2Br\\ |\\ Fe_xBr_n\end{array}\right]Br \quad \mathbf{3}$$

$$\text{(d)}\quad \text{solvated } \mathbf{3} \longrightarrow \left[\begin{array}{c}(C_6H_5)_2C{-}CHBr\\ |\qquad\ \ \vdots\\ Br_nFe_x\cdots H\end{array}\right]Br \quad \mathbf{4}$$

$$\text{(e)}\quad \mathbf{4} \longrightarrow (C_6H_5)_2C{=}CHBr + HBr + Fe_xBr_n$$

revealed four multiplets centered at amu 414, 494, 574, and 654, respectively. The corresponding parent compounds would have the following composition $[Fe(R)(Br)_n(H_2O)]$, where R = $(C_6H_5)_2CCH_2Br$ and n = 1–4. The H_2O coordinate molecule would come from the silica gel.

The mass spectra of fractions 8–9 show multiplets centered at amu 370, 372, 450, 452, 530, 609, and 611. The assigned compositions are $[Fe_2(R)(Br)_n]$, where R = $(C_6H_5)_2CCH_2Br$ and n = 0–3. The main peaks in the mass spectra are those from the organic moiety.

Fractions 4–9 show a relative high iron signal by atomic absorption spectrophotometry.

The isolated organoiron compounds are indeed the most stable, but they are not necessarily the most important ones from the quantitative or mechanistic point of view.

Acknowledgment. We thank the Consejo Nacional de Investigaciones Científicas y Técnicas (CONICET)-Argentina and the Consejo de Investigaciones de la Provincia de Córdoba (CONICOR) of Córdoba, Argentina, for financial support. We also thank Lic. José Indovino for assistance in iron particle diameter measurements with a scanning electron microscope Phillips (SEM) 501 B. and Lic. Pedro Contreras for iron determinations with a Perkin Elmer 372 atomic absorption spectrometer.

Registry No. 1, 40957-21-9; **2**, 13249-58-6; Fe, 7439-89-6.

---

[6] (a) Mc. Elvany, S. W.; Allison, J. *Organometallics* **1986**, *5*, 416. (b) Mc. Elvany, S. W.; Allison, J. *Organometallics* **1986**, *5*, 1219.

[7] Allison, J.; Ridge, D. P. *J. Am. Chem. Soc.* **1976**, *98*, 7445.

[8] Ashby, E. C.; Wiesemann, T. L. *J. Am. Chem. Soc.* **1978**, *100*, 189.